Disappearance of Shell Effects at High Excitation. *Self-consistent Calculations at Finite Temperatures*

1974 Phys. Scr. 10 163

(http://iopscience.iop.org/1402-4896/10/A/028)

Physica Scripta. Vol. 10 A, 163–169, 1974

Disappearance of Shell Effects at High Excitation

Self-consistent Calculations at Finite Temperatures

M. Brack and Ph. Quentin[1]

The Niels Bohr Institute, University of Copenhagen, Copenhagen, Denmark

Received July 23, 1974

Abstract

Disappearance of shell effects at high excitation: Self-consistent calculations at finite temperatures. M. Brack and Ph. Quentin (The Niels Bohr Institute, University of Copenhagen, Copenhagen, Denmark).
Physica Scripta (Sweden) 10 A, 163–169, 1974.

Self-consistent calculations of highly excited nuclei are presented. The changes in the average nuclear field as a function of temperature are discussed; they are found to be negligible in the calculation of the entropy versus excitation energy at a fixed deformation. The disappearance of shell effects at temperatures $T \simeq 2$–3 MeV in heavy nuclei is demonstrated both by calculations of deformation energy curves at different temperatures and by considering the asymptotic behaviour of the entropy. Finally, the validity of some simplifying approximations is discussed.

1. Introduction

As is well known, the problem of the stability of superheavy nuclei against fission decay is dominated by the existence of strong shell effects [1]. On the other hand, shell effects disappear at high excitation [2, 3]. Therefore, in discussing the possibility of producing superheavy elements, it is of importance to make predictions of level densities of highly excited heavy nuclei. Such calculations have been done by different groups [4] within the statistical model using the spectra of independent particles moving in a deformed average nuclear potential. The deformation probability of the nucleus is determined by first calculating the deformation energy surface with the Strutinsky method [2, 5] and then evaluating the level density as a function of excitation and of deformation. This approach is not self-consistent, and one might ask to what extent the parameters of the average field and of the liquid drop model should depend on the temperature. This gives the motivation for approaching the calculation of excitation energies and level densities in a self-consistent way. Indeed, in such a calculation, one derives simultaneously the average potentials, single particle states and occupation probabilities at each temperature. Calculations along these lines have recently been undertaken for medium and light nuclei [6] and for heavy nuclei [7]. The results presented here are a continuation of the calculations reported in ref. [7].

2. Theory

The Hartree-Fock (HF) approximation at finite temperature can be found in different textbooks [8]. Here we restrict ourselves to a short presentation of the most important formulae. Starting from a Hamiltonian H with a nuclear interaction $\mathcal{V}$

$$\mathcal{V} = v^{(2)} + v^{(3)} + \ldots, \tag{1}$$

where the part $v^{(p)}$ acts between p particles, one has to solve the coupled system of equations

$$H(\varrho)\varphi_i(\boldsymbol{r}) = \varepsilon_i \varphi_i(\boldsymbol{r}), \tag{2a}$$

$$\mathrm{Tr}\,\varrho = \sum_i f_i = N. \tag{2b}$$

The one-body Hamiltonian $H(\varrho)$ is determined as in usual HF-theory; but now it depends on the temperature through the density matrix ϱ which in terms of an arbitrary basis $|\alpha\rangle$ has the form

$$\varrho_{\alpha\beta} = \sum_i f_i \langle\alpha|i\rangle\langle i|\beta\rangle. \tag{3}$$

In these equations, N is the particle number and f_i are the statistical Fermi occupation probabilities

$$f_i = [1 + \exp\{\beta(\varepsilon_i - \mu)\}]^{-1}; \tag{4}$$

β is the inverse temperature ($\beta = 1/kT$) and μ the chemical potential. The HF-equations (2a, b) are derived by minimizing the thermodynamic potential Ω:

$$\delta\Omega = \delta(E - TS - \mu N) = 0. \tag{5}$$

Hereby, the variation of the wave functions $\varphi_i(\boldsymbol{r})$ (i.e. the coefficients $\langle\alpha|i\rangle$) leads to eq. (2a); the variation of the occupation numbers f_i leads to eq. (2b). In eq. (5), E is the average nuclear energy

$$E = \langle\mathcal{T} + \mathcal{V}\rangle = \sum_i f_i \varepsilon_i - \sum_p (p-1)\langle v^{(p)}\rangle \tag{6}$$

and S the entropy

$$S = -\sum_i \{f_i \ln f_i + (1-f_i)\ln(1-f_i)\}. \tag{7}$$

The excitation energy $E^*(T)$ at a given temperature is defined by

$$E^*(T) = E(T) - E(0). \tag{8}$$

For simplicity, we have presented the formalism without inclusion of pairing correlations. These are important only at low temperatures ($T \lesssim 1$ MeV); since we are interested in high excitations here, we always consider temperatures for which the BCS gaps are zero ($T \geqslant 1$ MeV). For the evaluation of the ground state energies ($T = 0$), however, we do include the pairing effects. This is done self-consistently within the BCS approximation, as described in ref. [9], using constant pairing strengths G_n and G_p (see the case of ^{168}Yb below).

3. Numerical details

We have solved the HF-equations (2a, b) for some selected nuclei in different mass regions: ^{40}Ca, ^{168}Yb, ^{208}Pb and the hypothetical

[1] Permanent address: Division de Physique Théorique, IPN Orsay, France.

Table I. *Proton single particle energies ε_i obtained for $^{298}_{114}Gg$ in the two different codes (only upper part of the spectrum). The horizontal line corresponds to the Fermi energy at $T=0$*

State	Deformed code $T=0$	Spherical code $T=0$	Spherical code $T=5$ MeV
$1h_{11/2}$	−12.47	−12.34	−12.94
$2d_{3/2}$	−11.91	−11.89	−12.24
$3s_{1/2}$	−11.14	−11.00	−10.87
$1h_{9/2}$	− 8.73	− 8.60	− 9.54
$1i_{13/2}$	− 5.62	− 5.45	− 6.17
$2f_{7/2}$	− 5.60	− 5.44	− 5.84
$2f_{5/2}$	− 3.73	− 3.51	− 4.27
$3p_{3/2}$	− 2.80	− 2.65	− 2.55
$3p_{1/2}$	− 2.18	− 2.01	− 2.05
$1i_{11/2}$	− 0.44	− 0.26	− 1.44
$1j_{15/2}$	1.60	1.80	0.99
$2g_{9/2}$	2.24	2.50	1.88
$2g_{7/2}$	4.57	4.93	3.93
$3d_{5/2}$	6.27	6.30	5.83
$3d_{3/2}$	7.04	7.08	6.57
$4s_{1/2}$	8.13	8.11	7.39
$1j_{13/2}$	8.30	8.51	7.10
$1k_{17/2}$	9.11	9.34	8.48
$2h_{11/2}$	10.67	10.67	9.81
$2h_{9/2}$	13.25	13.25	12.12
$3f_{7/2}$	15.95	14.57	13.64
$3f_{5/2}$	16.95	—	—
$1k_{15/2}$	17.20	17.48	15.89
$4p_{3/2}$	18.16	—	—
$1l_{19/2}$	18.25	17.21	16.25
$4p_{1/2}$	18.69	—	—
$2i_{13/2}$	19.05	18.70	17.59

superheavy nucleus $^{298}_{114}$Gg.[1] The temperature was varied from $T=0$ to $T=6$ MeV. For the interaction we used the effective interaction of Skyrme which has been very successful in describing nuclear properties as binding energies, radii and deformations [9, 10]. We have chosen the set of parameters SIII which was used in recent extensive calculations [11]. As already pointed out in ref. [7], we have to make the assumption that the temperature dependence of the effective interaction can be neglected.

The analytical simplicity of the Skyrme interaction leads to a set of *differential* equations (2a) instead of the usual integro-differential system. The practical solution of these equations depends on the imposed symmetry of the nucleus. For spherical nuclei, we solve eq. (2a) in coordinate space.[2] For axially symmetric deformations, we use an improved version of the code by Vautherin [9] for diagonalization of the matrix $H(\varrho)$ in a truncated deformed harmonic oscillator basis. As a shorthand notation, we will refer to the two codes as the "spherical" and the "deformed" code, respectively (although the latter can be used for spherical nuclei as well).

For temperatures $T \gtrsim 2.5$–3 MeV, a problem arises due to the non-negligible contributions from the continuum region, as is the case for Strutinsky calculations with a finite depth potential [2]. When using the deformed code, we simply include the unbound levels obtained by the matrix diagonalization. Similarly in the spherical code, we use in an approximate way those states which are "quasibound" by their Coulomb and centrifugal barriers. This prescription of course only provides a limited number of high-lying states, in contrast to the deformed case. We checked that for a sufficiently large basis in the deformed code, the single particle spectra given by the two codes are closely the same also in the continuum region. This is demonstrated in Table I for the proton spectra of ^{298}Gg. In the first two columns we compare the spectra (at $T=0$) around the Fermi level (indicated by the horizontal line) as they are obtained in the two codes. The bound states agree within ~0.2 MeV;[3] those unbound states which lie below +14 MeV agree within less than ~0.4 MeV. A similar agreement was found in the spectra of ^{208}Pb, for neutrons as well as for protons. The missing of higher unbound states in the spherical code starts affecting the results for $T \gtrsim 2.5$ MeV.

In the deformed code, on the other hand, one faces the additional problem of optimizing the parameters of the truncated basis. This optimization is done by minimizing the free energy $F=E-TS$ at each temperature; however, it becomes more and more critical with increasing temperature. For the nucleus ^{168}Yb, e.g., a basis with 11 oscillator shells, which is sufficiently large at $T=0$, was found to be too small for a reliable optimization above $T \simeq 4$ MeV.

We have checked quantitatively the continuum and truncation effects on the excitation energies E^* and entropies S by comparing the results obtained for ^{208}Pb with the two different codes (13 shells were included in the basis). We found that both E^* and S obtained in the two different ways agree within 1% up to $T=2.5$ MeV ($E^*=110$ MeV). For $T \gtrsim 2.5$ MeV, the results start deviating. A consequence of this will be seen in Fig. 7 below. Otherwise, it does not affect the conclusions drawn in this paper.

At temperatures for which the occupation probabilities of unbound states are sufficiently large, the evaporation of nucleons becomes physically important. We do not, however, take this process into account, since it cannot be described by equilibrium statistics. Therefore, our results at very high temperatures ($T \sim 5$–6 MeV) should only be used for asymptotic extrapolations (see the discussion after eqs. (9)–(11) below) and are not meant to describe any real physical systems. One should also keep in mind that the particle number is only conserved, on the average, by eq. (2b). As an example, the fluctuation $\langle (N-\langle N\rangle)^2\rangle^{\frac{1}{2}}$ for ^{168}Yb at $T=3$ MeV is 3.69 and 3.25 for neutrons ($N=98$) and protons ($Z=70$), respectively.

4. Results

We found in ref. [7] that the selfconsistent single particle levels ε_i of ^{208}Pb vary only slightly with temperature (see figure 1 of ref. [7]). The same was observed in all spherical nuclei considered. As a rule, the lowest levels increase slightly with temperature, whereas high-lying states decrease. The strongest variation between $T=0$ and $T=5$ MeV did not exceed ~1.6 MeV. This holds good for both proton and neutron levels. As a further example, we have listed part of the proton spectrum of ^{298}Gg at $T=0$ and $T=5$ MeV in columns 2 and 3 of Table I.

This remarkable constancy can be understood qualitatively by looking at the behaviour of the local potentials and the effective masses of the Skyrme-HF-Hamiltonian (see ref. [10]) as functions of the temperature. Since these quantities are self-consistently related to the density distributions, we first present as an example in Fig. 1 the proton density distributions of ^{208}Pb at three different temperatures. We see that the heating of the system results in a smoothing of the shell oscillations; at $T=5$ MeV the distribution is almost perfectly smooth. At the same time the central density is clearly lowered and the surface region is broadened. This trend, which leads to an increase of the root mean square radius, can easily be understood by the inclusion of higher lying states with larger quantum numbers as the temperature grows.

[1] Gg = Gammelgormium (name not officially approved).

[2] We are grateful to M. Beiner and H. Flocard for providing us with an improved version of the code by Vautherin and Brink [10].

[3] This difference is due to the truncation; the numerical error in the energies ε_i is one order of magnitude smaller.

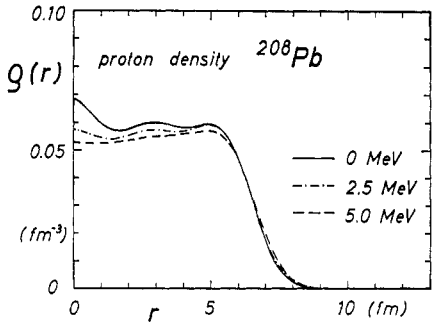

Fig. 1. Self-consistent proton density distributions $\varrho_p(r)$ of ^{208}Pb at three temperatures.

The increase of the smooth proton density with the radius is mainly a Coulomb effect[1] and almost non-existent in the corresponding neutron distribution.

The smooth density seen in Fig. 1 at $T=5$ MeV might be compared to the one obtained from the self-consistent density by a Strutinsky averaging [2, 12]. This averaging, however, leads to a "cold" average density (see also ref. [13]) as compared with the "hot" one in Fig. 1, and therefore the two smooth distributions have different features. The cold average density still contains some remaining oscillations which are connected to the Friedel oscillations [14]; its root mean square radius is *not* larger than the self-consistent one. In the heated distribution (Fig. 1), the Friedel oscillations are much less pronounced due to the increased surface thickness. A more detailed comparison of the two averaging processes will be found elsewhere [15].

The proton and neutron r.m.s. radii of ^{208}Pb are shown in Fig. 2 as functions of the temperature. Fig. 3*a* shows the proton effective mass $m_p^*(r)$ in units of m_0 and Fig. 3*b* the local proton potential $U_p(r)$ (including the Coulomb potential) of the same nucleus. The increase of the effective mass and the decrease of the density $\varrho_p(r)$ inside the nucleus are directly connected (see the definition of $m^*(r)$ in ref. [10]). The radius of the potential $U_p(r)$ increases with temperature at the same rate as that of the density $\varrho_p(r)$, whereas its average depth seems almost constant or to decrease only very slightly.

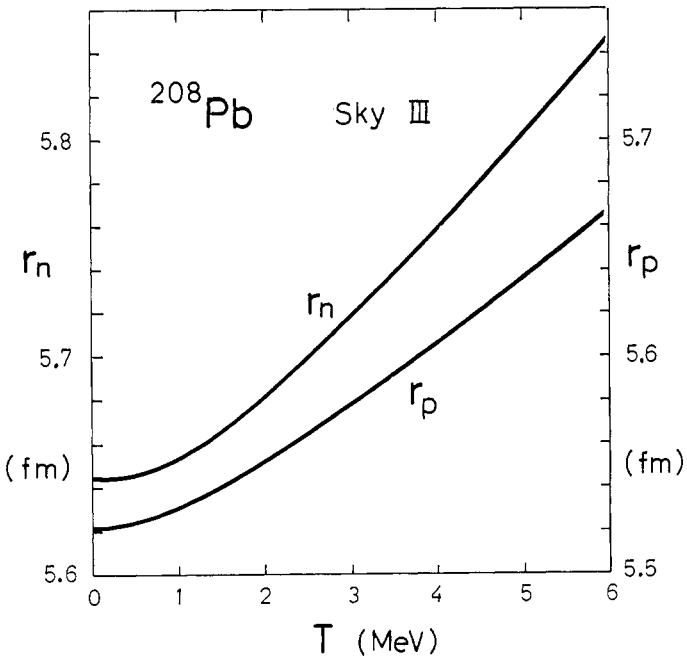

Fig. 2. Proton and neutron root-mean-square radii of ^{208}Pb as functions of temperature. Note the different scales on the left and right sides.

[1] We are grateful to Professor W. Swiatecki for drawing our attention to this point.

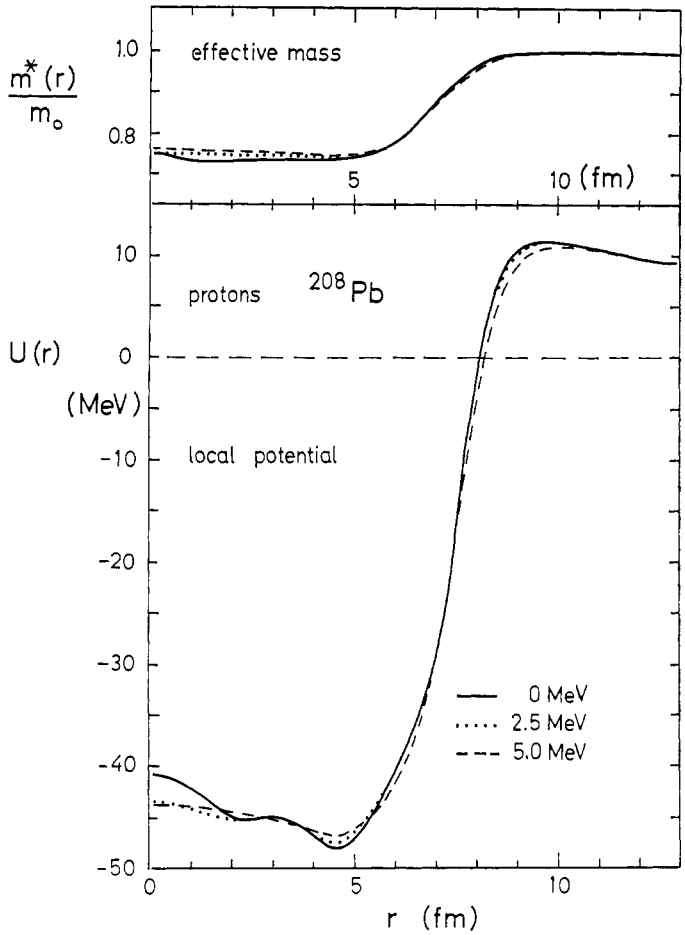

Fig. 3. Properties of the proton single-particle HF Hamiltonian of ^{208}Pb at three temperatures. (*a*) Upper part: Effective mass $m_p^*(r)$ in units of the free proton mass m_0. (*b*) Lower part: Local proton potential $U_p(r)$ including the Coulomb potential.

The effect of these variations on the single particle spectrum is now the following: An increase of the effective mass raises the deep-lying levels and lowers the high-lying ones (see, e.g. ref. [11]). An increase of the radius, on the other hand, lowers the entire spectrum. These two effects cancel each other in the lower part of the spectrum and go in the same direction for the high-lying states. This explains in a qualitative way the results described above for the temperature dependence of the single-particle spectra.

A consequence of the small variation of the single-particle levels with temperature is that one can use the *fixed* ground state spectrum (at $T=0$) to obtain the entropy of the nucleus as function of its excitation energy in a very good approximation. This has been demonstrated for the case of ^{208}Pb in ref. [7] and will be discussed further in Sect. 5 below.

In nuclei with a deformed ground state, we have to expect more changes of the average field, since the melting of the shell structure will make the nucleus spherical at high excitation. We demonstrate this in Fig. 4 where we have plotted the free energy $F=E-TS$ versus the mass quadrupole moment Q_2 of the nucleus ^{168}Yb at various temperatures ($T=0$, 1, 2, 3 MeV). These curves are obtained with a quadratic constraint on the quadrupole moment (see Flocard et al. [9]). The local minima, indicated by circles, can of course be obtained without constraint. At $T=0$, the pairing effects were included as described in ref. [11]; the constant pairing strengths $G_p=0.19$ MeV and $G_n=0.15$ MeV were

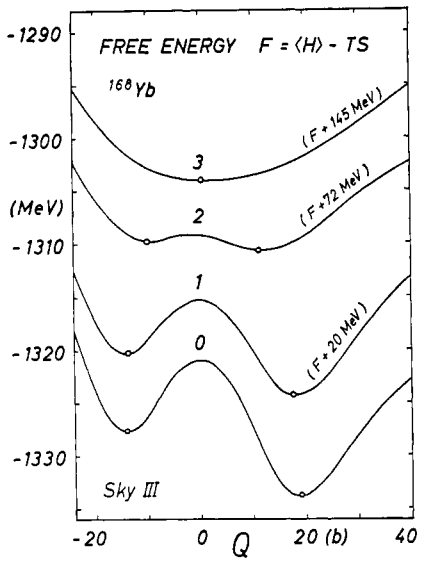

Fig. 4. Potential (free) energy of ^{168}Yb versus mass quadrupole moment at different temperatures ($T=0$, 1, 2, 3 MeV). The curves with $T>0$ are shifted upwards by the amount indicated in parentheses. Pairing included (see text).

determined by the constant uniform gap method proposed by Strutinsky [5, 2] ($\tilde{\Delta}=1$ MeV). We checked that the critical temperature T_c at which the gaps disappear is less than 1 MeV at all deformations considered. The basis contained 11 oscillator shells and its parameters were optimized at all points. The convergence of the results was checked by including 13 shells for some points.

As expected, the shell effects in the curves of Fig. 4 disappear with increasing excitation. At $T\simeq 3$ MeV, the deformation energy curve behaves like a liquid drop model curve. In particular, the minimum is at zero quadrupole moment. Fig. 5 shows that also the hexadecapole moment Q_4 vanishes at the same rate as Q_2, thus really leading to a spherical shape at $T\simeq 3$ MeV. The curves $Q_2(T)$, $Q_4(T)$ in this figure were obtained from the solutions at the local minima (circles in Fig. 4) on the prolate side. At temperatures $T\gtrsim 4$ MeV, the quadrupole moment Q_2 is numerically not exactly zero but has values which lie within the hatched area in Fig. 5. This is due to the truncation effects mentioned above and has no physical significance.

Of course, our approach is purely static; a proper inclusion of dynamics which would allow collective vibrations of the nucleus could easily lead to an average spherical shape already

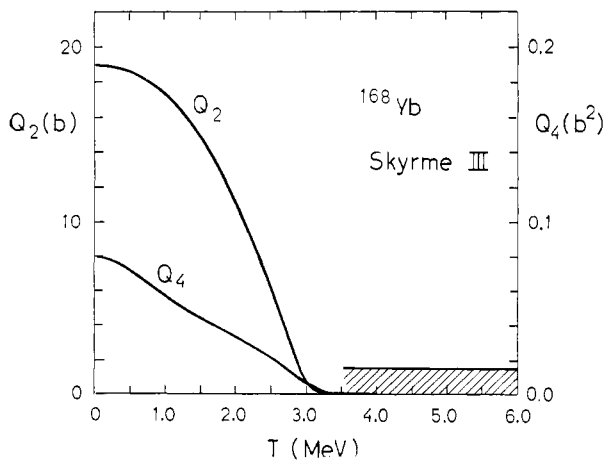

Fig. 5. Mass quadrupole and hexadecapole moments of ^{168}Yb at the equilibrium deformations versus temperature (see text for the meaning of the shaded area).

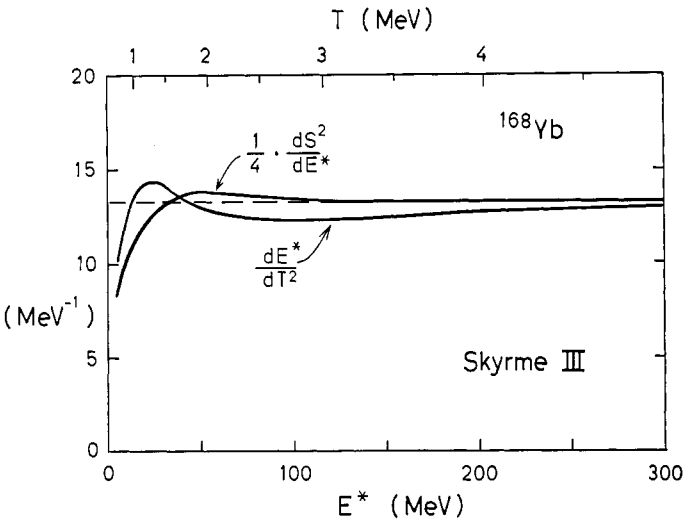

Fig. 6. Asymptotic behaviour of

$$\frac{dE^*}{dT^2} \text{ and } \frac{1}{4}\frac{dS^2}{dE^*}$$

of ^{168}Yb as functions of excitation energy. The horizontal (— —) line corresponds to the value of the level density parameter a, eq. (11).

at $T\simeq 2$ MeV, due to the softness of the central barrier of the curve $F(Q_2)$ (Fig. 4) at this temperature.

The disappearance of the shell effects can also be seen when studying the entropy as a function of excitation energy. At temperatures which are high enough to wipe out the shell effects, the entropy S and the excitation energy E^* are approximately given by the asymptotic formulae (see e.g. [4])

$$\left.\begin{aligned} S &\sim 2\sqrt{a(E^*+\Delta E_0)} \\ E^* &\sim aT^2-\Delta E_0. \end{aligned}\right\} \quad (E^*\gg\Delta E_0) \tag{9, 10}$$

Here ΔE_0 is the ground state shell-correction and a the level density parameter which is proportional to the average density $\tilde{g}(\mu)$ of single particle states ε_i at the Fermi energy:

$$a=\frac{\pi^2}{6}\tilde{g}(\mu). \tag{11}$$

We can check the asymptotic relations (9, 10) by looking at the quantities

$$\frac{1}{4}\frac{dS^2}{dE^*}\equiv\frac{S}{2T} \quad \text{and} \quad \frac{dE^*}{dT^2}$$

evaluated numerically from the finite differences obtained at different temperatures. Fig. 6 shows these quantities for ^{168}Yb as functions of E^*. The horizontal dashed line corresponds to the value a as found from the ground state spectrum by means of a Strutinsky procedure. We see that $\frac{1}{4}\frac{dS^2}{dE^*}$ reaches exactly the value a at $T\simeq 3$ MeV. The quantity $\frac{dE^*}{dT^2}$ is also approximately constant for $T\gtrsim 2.5$ MeV, but with a somewhat smaller value than a. The reason for this is that the derivatives $\tilde{g}'(\mu)$, $\tilde{g}''(\mu)$, etc. of the average single particle level density, which are non-zero in realistic cases, have been neglected in eqs. (9, 10); it appears that they affect eq. (9) much less than eq. (10).

The behaviour of the curves in Fig. 6 at low temperatures reflects the shell structure. Such plots can therefore be used to

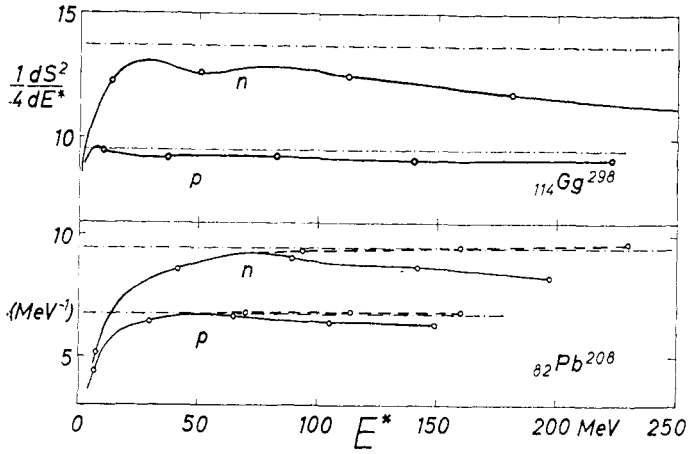

Fig. 7. The quantity $\frac{1}{4}\frac{dS^2}{dE^*}$ as in Fig. 6, but separately for neutrons and protons for the nuclei ^{208}Pb and $^{298}_{114}$Gg. Solid lines obtained with the spherical code, dashed lines (for ^{208}Pb) obtained with the deformed code. The circles correspond to the temperatures $T=1$, 2, 3, 4, 5 MeV.

approximately determine the temperature (excitation energy) at which the shell effects disappear.

In Fig. 7 we present similar plots of $\frac{1}{4}\frac{dS^2}{dE^*}$ for the nuclei ^{208}Pb and ^{298}Gg. Since it is interesting to study the contributions from neutrons and protons separately, we have evaluated S, E^* and the derivative $\frac{1}{4}\frac{dS^2}{dE^*}$ for each kind of nucleons. For the excitation energy E^*, this separation into two parts is not trivial, since the potential energy term in the total HF-energy, eq. (6), couples the neutron and proton contributions. However, the approximations to E^* discussed in Sect. 5 below allow to separate the two contributions.

As in Fig. 6, the horizontal (–·–) lines in Fig. 7 correspond to the values of the level density parameter a evaluated from the ground state spectra ε_i. The solid curves are the quantities $\frac{1}{4}\frac{dS^2}{dE^*}$ calculated with the spherical code. In the case of ^{208}Pb, we show by dashed curves the results calculated with the deformed code. The deviations at $T\gtrsim 3$ MeV are due to the different treatment of the continuum region discussed above. The asymptotic behaviour found with the deformed code is clearly better because of the larger number of unbound states included. The difference is, however, smaller for protons due to the Coulomb barrier. The quantities $\frac{1}{4}\frac{dS^2}{dE^*}$ reach the values a within ~2% for ^{208}Pb and ~4% for ^{298}Gg. The fact that these values of a are the ones found from the ground state spectra once more demonstrates the smallness of the change of the spectrum with temperature.

Obviously the shell effects are stronger in ^{208}Pb than in the superheavy nucleus. In the former case the asymptotic values of a are reached at $T\simeq 2.5$ MeV, whereas in the latter nucleus this is the case already at $T\simeq 1.5$–2 MeV. For completeness we give the total quantities S, E^* and $\frac{1}{4}\frac{dS^2}{dE^*}$ evaluated for ^{298}Gg at temperatures $T=0.5$ MeV to 5 MeV in Table II. We can conclude that for this nucleus an excitation energy E^* of 25–30 MeV seems sufficient to destroy the shell effects. This estimate is however subject to different limitations and several improvements have to be made before one can give a more accurate number. First, one should calculate the entire deformation energy curve (as in Fig. 4 for ^{168}Yb) as a function of temperature in order to consider the effect on the whole fission barrier (see ref. [16]). Second, as we mentioned above, collective vibrations become more important when the deformation energy curve is smoothed out. Third, the effect of rotations may not be neglected, as high spins also tend to lower the shell effects (see ref. [17]). The spin could be taken into account by inclusion of some constraint in the HF-equation; for very heavy nuclei such a calculation exceeds, however, the limits of computer time available at present.

5. Approximations to excitation energy and entropy

As already mentioned in ref. [7], the excitation energy E^* (8) and the entropy S (7) can be obtained in a very good approximation by using the level spectra $\varepsilon_i^{(0)}$ obtained at $T=0$, i.e. by defining

$$E^{*(0)}=\sum_i f_i^{(0)}\varepsilon_i^{(0)}-\sum_{i=1}^{N}\varepsilon_i^{(0)}, \tag{12}$$

$$S^{(0)}=-\sum_i\{f_i^{(0)}\ln f_i^{(0)}+(1-f_i^{(0)})\ln(1-f_i^{(0)})\}, \tag{13}$$

where $f_i^{(0)}$ are defined as in eq. (4) in terms of the $\varepsilon_i^{(0)}$. In other words the variation of the single particle wavefunctions $\varphi_i(\boldsymbol{r})$, i.e. the solution of eq. (2a), is omitted for $T\neq 0$ and only eq. (2b) is solved at each temperature. This approximation corresponds exactly to the non-selfconsistent approaches [4], if the $\varepsilon_i^{(0)}$ are identified with the levels obtained in the phenomenological average potentials. As demonstrated in figure 2 of ref. [7] for the case of ^{208}Pb, the values of $E^{*(0)}$ and $S^{(0)}$ start deviating from the self-consistent ones at $T\gtrsim 2$ MeV, but in such a way that the two functions $S(E^*)$ and $S^{(0)}(E^{*(0)})$ remain the same up to $T=6$ MeV. Thus the approximation (12, 13) leads to a slight redefinition of the temperature, without however affecting the quantity of physical interest, namely the entropy as function of excitation, within the numerical accuracy of the calculations. The same result was also obtained for the nuclei ^{40}Ca[1] and ^{298}Gg.

The approximation (12, 13) can be used in deformed nuclei, too. But here one has to keep the deformation fixed at each temperature by using a constraint. Otherwise the average poten-

Table II. *Excitation energy E^*, entropy S and effective level density parameter $\frac{1}{4}\frac{dS^2}{dE^*}$ obtained for $^{298}_{114}$Gg at different temperatures T (spherical code used)*

T (MeV)	E^* (MeV)	S	$\frac{1}{4}\frac{dS^2}{dE^*}$ (MeV^{-1})
0.5	6.4	19.8	19.8
1.0	23.7	43.4	21.7
1.5	51.7	66.5	22.2
2.0	87.7	86.6	21.4
2.5	137.8	109.8	21.7
3.0	194.3	130.6	21.3
3.5	253.6	149.0	21.0
4.0	321.6	167.5	20.9
4.5	397.4	185.7	20.6
5.0	478.5	203.2	20.3

[1] We should point out that our results for ^{40}Ca contradict those found by the authors of ref. [6]. Their results show a strong variation of the levels with temperature and a rather large discrepancy between the curves $S(E^*)$ and $S^{(0)}(E^{*(0)})$ for $T\gtrsim 2$ MeV. It should be stressed that we did the calculations for ^{40}Ca with the spherical code which eliminates possible error sources due to truncation and optimization of the basis.

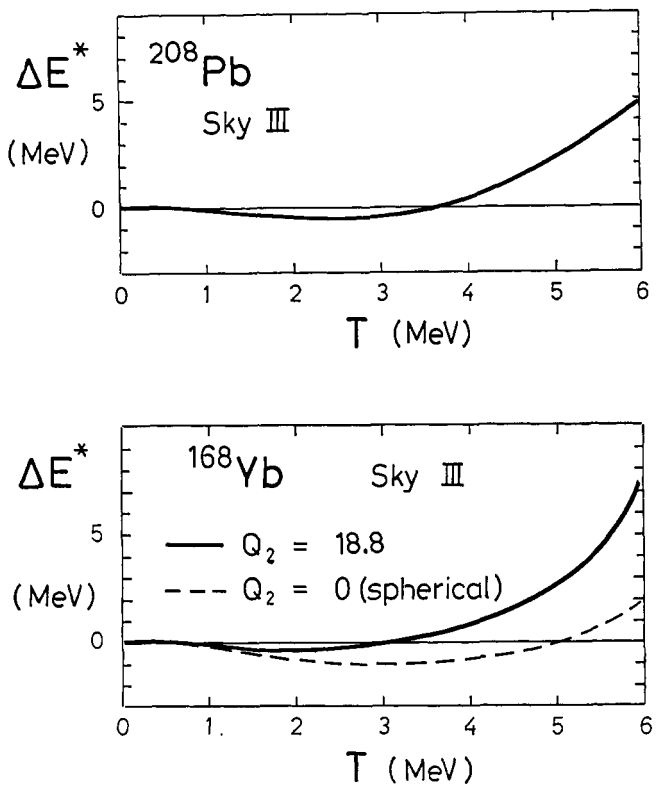

Fig. 8. Difference between exact excitation energy E^* eq. (8) and the approximation $E^{*\prime}$ eq. (14) as function of temperature. Upper case: ^{208}Pb (with spherical code). Lower case: ^{168}Yb at two fixed deformations (see text). Case $Q_2 = 18.8$b obtained with deformed code, case $Q_2 = 0$ with spherical code. In both of these cases the pairing energy at $T = 0$ has been added to eq. (14).

tial changes its shape with increasing temperature, as shown in Figs. 4 and 5, which leads to a substantial rearrangement of the levels ε_i and therefore strongly affects both S and E^*. For a fixed deformation[1] however, the levels ε_i vary with temperature as little as in spherical nuclei, and the approximation (12, 13) leads for ^{168}Yb to similar results as those found in the spherical nuclei.

In order to take the pairing effects into account, one has to modify eqs. (12, 13) by replacing the occupation numbers $f_i^{(0)}$ by the temperature dependent BCS occupation numbers and by adding to $E^{*(0)}$ the difference in pairing energies at the temperatures T and zero (see, e.g. Moretto [4]).

Another approximation to the self-consistent excitation energy E^*, which may be of more academic than practical interest, is given by

$$E^{*\prime} = \sum_i f_i^{(T)} \varepsilon_i^{(T)} - \sum_{i=1}^{N} \varepsilon_i^{(T)}, \tag{14}$$

where $\varepsilon_i^{(T)}$ and $f_i^{(T)}$ are the selfconsistent quantities evaluated at the temperature T; again the deformation is to be fixed by a constraint for all values of T. We found that $E^{*\prime}$ eq. (14) approximates the exact value of E^* to within ~ 1 MeV up to $T \simeq 4$ MeV in heavy nuclei; in ^{208}Pb this corresponds to a relative accuracy of 0.4% at $T = 4$ MeV. The difference $\Delta E^* = E^* - E^{*\prime}$ is plotted in Fig. 8 for ^{208}Pb and for ^{168}Yb at two fixed deformations.

[1] For the case of ^{168}Yb at the ground state deformation ($Q_2 = 18$ barns), it turned out to be sufficient to constrain the quadrupole moment Q_2 for $T > 0$; the hexadecapole moment Q_4 stays constant within $\sim 20\%$ at all temperatures. This is explained by the fact that the deformation (Q_2, Q_4) of the ground state of this special nucleus lies close to the liquid drop valley of the smooth deformation energy surface which is approximated at high temperature.

The smallness of the difference ΔE^* can be explained using an argument which is formally the same as the one used for the derivation of the Strutinsky energy theorem [2, 5, 12] from HF theory. For not too high temperatures, the difference $\delta\varrho = \varrho_T - \varrho_0$ between the self-consistent density matrices at temperatures T and zero is relatively small, i.e. $|\delta\varrho| < |\varrho_0|$ (see e.g. Fig. 1). (Here it is important that the moments Q_2, Q_4, ... of the density distributions $\varrho(r)$ are constrained to be constant for all temperatures.) One can therefore expand the HF-Hamiltonian $H(\varrho_T)$ (eq. (2a) including constraints) around ϱ_0 and treat the difference $H' = H(\varrho_T) - H(\varrho_0)$ as a small perturbation of $H(\varrho_0)$. It can then be shown in a straight-forward way, using first order perturbation theory, that the difference $\Delta E^* = E^* - E^{*\prime}$ is of *second order* in $\delta\varrho$; all contributions of first order in $\delta\varrho$, which come from the potential energy terms in the right hand side of eq. (6), are cancelled identically due to the stationary condition (5).

In a similar way one can show that the difference $E^* - E^{*(0)}$, eqs. (8, 12) is a second order quantity; however this is less straightforward since two different occupation numbers $f_i^{(T)}$ and $f_i^{(0)}$ are involved.

The simplified approximative expression for the excitation energy, eq. (14), is formally similar to the definition of E^* in the non-selfconsistent approach [4]. It might be used to generalize the considerations of Bhaduri and das Gupta [13] to the self-consistent HF case. Such investigations are in progress [15].

6. Conclusions

We have shown that the variation of the self-consistent average nuclear potentials with temperature affect the single particle levels ε_i only very little. For the evaluation of the entropy as a function of the excitation energy at a fixed deformation, the use of the ground state ($T = 0$) spectra leads therefore to almost identical results even at very high excitations. This result justifies *a posteriori* the non-selfconsistent approaches [4] in which the fixed spectra of phenomenological average potentials are used.

Our conclusion that the self-consistency effect at finite temperatures can be neglected, applies only to energy *differences* such as the excitation energy E^* and its relation to the entropy S. As the *total* energies E eq. (6) or $F = E - TS$ as functions of the temperature are concerned, the self-consistency of our approach is essential. A fit of the curves $F(Q)$ at $T \gtrsim 3$ MeV to a liquid drop model (LDM) expression might, for instance, allow determination of the temperature dependence of the LD-parameters inherent in the interaction used. In fact, a preliminary comparison of the curve $F(Q)$ at 3 MeV in Fig. 4 with the curve $\bar{E}(Q)$, found in ref. [12] from the HF energy at $T = 0$ by a Strutinsky averaging, seems to suggest a slight decrease of the surface energy coefficient with increasing temperature. A more detailed investigation will be presented in ref. [15].

The starting basis of all realistic level density calculations quoted in ref. [4] is the evaluation of a deformation energy surface by means of Strutinsky's shell-correction method [5]. In ref. [12], we have shown numerically that the Strutinsky method is consistent with the constrained HF method up to fluctuations of the order of $\pm \sim 1$ MeV in the total energy of a heavy nucleus. We have recently extended these calculations to the use of a different effective interaction and thereby confirmed the previous conclusions [18].

Together with the present results, we have thus given theoretical support to the entire non-selfconsistent statistical approach [4] to high nuclear excitations. Our further investigations [15] aim at a determination of the "ideal" average potential and LD para-

meters to be used in this approach as an alternative to the much more complicated and time-consuming, temperature-dependent, constrained HF method.

Acknowledgement

The authors are grateful to Professor M. Vénéroni, Dr S. Bjørnholm and Dr A. S. Jensen for enlightening discussions. The hospitality extended at the Niels Bohr Institute together with the support from the Japan World Exposition Commemorative Fund is gratefully acknowledged.

References

1. See, e.g., Myers, W. D. and Swiatecki, W. J., Nucl. Phys. **81**, 1 (1966).
2. Brack, M., Damgaard, J., Jensen, A. S., Pauli, H. C., Strutinsky, V. M. and Wong, C. Y., Rev. Mod. Phys. **44**, 320 (1972).
3. Bohr, A. and Mottelson, B., Nuclear Structure, Vol. II, to be published.
4. Ramamurthy, V. S., Kapoor, S. S. and Kataria, S. K., Phys. Rev. Lett. **25**, 386 (1970); Moretto, L. G., Nucl. Phys. **A182**, 641 (1972); Huizenga, J. R. and Moretto, L. G., Ann. Rev. Nucl. Sci. **22**, 427 (1972); Jensen, A. S. and Damgaard, J., Nucl. Phys. **A210**, 282 (1973); Døssing, T. and Jensen, A. S., Nucl. Phys. **A222**, 493 (1974).
5. Strutinsky, V. M., Nucl. Phys. **A95**, 420 (1967); **A122**, 1 (1968).
6. Mosel, U., Zint, P. G. and Passler, K. H. Preprint. Giessen University (1974).
7. Brack, M. and Quentin, P., Phys. Lett. **52 B**, 159 (1974). 1974).
8. See, e.g., Thouless, D. J., The Quantum Mechanics of Many Body Systems. Academic Press, 1961; Des Cloizeaux, J., *in* Many Body Physics, Les Houches 1967 (eds. C. de Witt and R. Balian); Gordon and Breach, 1968.
9. Vautherin, D., Phys. Rev. **C7**, 296 (1973); Flocard, H., Quentin, P., Kerman, A. K. and Vautherin, D., Nucl. Phys. **A203**, 433 (1973).
10. Vautherin, D. and Brink, D., Phys. Rev. **C5**, 626 (1972).
11. Beiner, M., Flocard, H., Quentin, P. and Nguyen Van Giai, to be published in Nucl. Phys.; see also references quoted therein.
12. Brack, M. and Quentin, P., Proc. III. IAEA Symposium on Phys. and Chem. of Fission, Rochester 1973, Vol. I, p. 231. IAEA Vienna, 1974.
13. Bhaduri, R. K. and Das Gupta, S., Phys. Lett. **47B**, 129 (1973).
14. Kohn, W. and Sham, L. J., Phys. Rev. **137**, A1697 (1965); see also Siemens, P. J., Phys. Rev. **C1**, 98 (1970).
15. Brack, M. and Quentin, P., to be published.
16. Beiner, M., Flocard, H., Vénéroni, M. and Quentin, P., contribution to this Symposium.
17. Bohr, A. and Mottelson, B., contribution to this Symposium.
18. Brack, M. and Quentin, P., Proc. Intern. Workshop II on Gross Properties of Nuclei and Nucl. Excitations, Hirschegg, p. 14. Techn. Hochschule Darmstadt, AED-Conf.-74-025-000 (1974).

The Niels Bohr Institute
University of Copenhagen
DK-2100 Copenhagen, Denmark

Discussion

Question: H. Meldner
Is it correct to conclude that these models suggest the approximate relation $E_{crit} = 3\ E_{shell}$ where E_{crit} denotes the critical excitation energy at which shell effects essentially disappear and E_{shell} is the shell correction?

Answer: M. Brack
Not if E_{shell} is the shell-correction to the liquid-drop energy (since E_{shell} might accidentally be zero). An upper estimate would probably be $T_{crit} = 1/2\ \hbar\Omega$, where $\hbar\Omega$ is the separation of the main shells around the Fermi level.

Question: H. S. Köhler
We have here seen a test of "Strutinsky" against a HF-calculation. However this correction is usually made using *observed* single-particle spectra. I would argue that one should use the single-particle energies *in the nucleus*. These are different from the observed ones that refer to a removal (or addition) of a nucleon. The difference is rearrangement. Without a fundamental theory I would guess that the Strutinsky method should really be applied to observed energies minus rearrangement energy (which is 5–10 MeV).

Answer: M. Brack
I agree with you. One should not use the observed single-particle spectra to obtain the shell-correction. Whether higher-order corrections (stemming from graphs not included in HF) to the single-particle levels or corrections due to correlations can be renormalized in Strutinsky's spirit, is an open question.

Question: C. F. Tsang
How is your result as to the second-order oscillating term, compared with that of Bassichis and Tuerpe?

Answer: M. Brack
The oscillating part of their higher-order terms is comparable to ours, taking into account the fact that they did not include pairing effects. The magnitude, however, is larger than ours and varies with the range of their averaging parameter, since they do not include what corresponds to Strutinsky's "curvature-corrections", when averaging the density matrix.